Structural Engineering and Mechanics, *Vol. 50, No. 5 (2014) 575-588*
DOI: http://dx.doi.org/10.12989/sem.2014.50.5.575

Mimicking the pattern formation of fruits and leaves using gel materials

Li Chen[1], Yang Zhang[1], Somsak Swaddiwudhipong[1a] and Zishun Liu[*2]

[1]*Department of Civil and Environmental Engineering, National University of Singapore, 117576, Singapore*
[2]*International Center for Applied Mechanics, State Key Laboratory for Strength and Vibration of Mechanical Structure, Xi'an Jiaotong University, Xi'an, 710049, China*

(Received December 5, 2013, Revised December 30, 2013, Accepted December 31, 2013)

Abstract. Gel materials have recently gained more attention due to its unique capability of large and reversible volumetric changes. This study explores the possibility of mimicking the pattern formation of certain natural fruits during their growing process and leaves during drying processes through the swelling and de-swelling of gel materials. This will hopefully provide certain technical explanations on the morphology of fruits and plants. We adopt the inhomogeneous field gel theory to predict the deformation configurations of gel structures to describe the morphology of natural fruits and plants. The growing processes of apple and capsicum are simulated by imposing appropriate boundary conditions and field loading via varying the chemical potential from their immature to mature stages. The drying processes of three types of leaves with different vein structures are also investigated. The simulations lead to promising results and demonstrate that pattern formation of fruits and plants may be described from mechanical perspective by the behavior of gel materials based on the inhomogeneous field theory.

Keywords: gel materials; inhomogeneous field theory; numerical simulation; pattern formation

1. Introduction

A three dimensional network can be formed by chemically linked, long chain polymer molecules. The resulting material exhibits the capability of large deformation under various stimuli including temperature, pH values, mechanical loads and ion changes. When solvent molecules are imbibed into the polymers, the system undergoes swelling instead of dissolution and such diluted material is referred to as gel (Horkay and McKenna 2007). Gel material is capable of large volumetric change due to the long flexible chains which extend throughout the network, providing the ability to undergo large and reversible deformations (Hong *et al*. 2009). Having such a unique feature, gel materials, especially hydrogels, are used for miscellaneous applications (Li *et al*. 2012). Hydrogels have been widely adopted as transporters in drug and protein delivery system (Censi *et al*. 2012). The materials can also be employed in tissue engineering as scaffold materials because of their biocompatibility with minimum inflammatory and tissue damage (Drury and Mooney 2003). A swelling elastomer packer has been used as a replacement for traditional

*Corresponding author, Professor, E-mail: zishunliu@gmail.com
[a]Professor, E-mail: ceesomsa@nus.edu.sg

http://www.techno-press.org/?journal=sem&subpage=8 ISSN: 1225-4568 (Print), 1598-6217 (Online)

mechanical packers and cement in oil exploration and production in recent years (Kleverlaan *et al*. 2005).

Fascinating patterns and shapes are often observed widely in nature. For example, fruits such as squash, small pumpkins and ridged gourds are observed to have ten longitudinal ridges while tomatoes and capsicums usually have just four (Yin *et al*. 2008). Such surface morphogenesis of fruits could be concluded as stress-driven patterns that may be considered as core/shell systems in modeling. Leaves on the other hand have shown intriguing deformation patterns as well (Liu *et al*. 2010). Different plants have displayed their distinctive venation patterns. For instance, a combination of mid-vein and lateral vein system is usually formed in dicot leaves while parallel pattern along the longitudinal axis is found in monocot leaves (Fujita and Mochizuki 2006). Such venation patterns may play an important role in the deformation of leaves during their growing and drying processes.

Although the origin of the pattern formation of natural fruits and plants are still unclear, several driving forces including genes (Green *et al*. 2010), chemistry and biophysics (Givnish 1987) and mechanics play certain roles in the growing and drying processes of fruits and plants (Dumais and Steele 2000, Liu *et al*. 2010, Liu *et al*. 2013).

A modeling study of morphological formation in melon was done by Chang *et al.* (2011) to try to characterize the pattern formation of melon with its cultivar, diameter and stripes and hence, predict the morphological growth of melon fruits. Yin *et al.* (2008, 2009) demonstrated that various fruit formation patterns might be manipulated by anisotropic stress-driven buckles on spheroidal system and examined the possibility of reproducing the surface undulations of fruits through their structures and geometric constrains. However, the sizes of mature stage of the fruits were used in the modeling, therefore, the effect of growing of the fruits was neglected and they adopted linearly elastic engineering material in the modeling. This might not be realistic enough because the deformation patterns of fruits during the growing and drying processes often involve relatively large volumetric changes. This prompted Liu *et al.* (2010, 2013) to adopt nonlinear inhomogeneous gel theory to study the deformation patterns of fruits involving the growing and drying processes.

While gel has been studied both experimentally and theoretically for more than a few decades, its complete understanding is still a challenge. As some behavior of gel under various external stimuli and boundary conditions is hard to be measured in laboratory, a better understanding may be reached via numerical simulations. The gel theory adopted in this article is based on Hong *et al.* (2009) and Liu *et al.* (2013). We adopt the relatively equivalent mechanical properties to those of fruit and leaf tissues that are currently available in the literature. Various types of natural fruits and leaves are numerically simulated and the configurations compared. In the simulation, the governing equations of gel deformation are implemented in the finite element package, ABAQUS, by using a user-defined subroutine for a hyperelastic material (UHYPER).

2. Principle of gel theory and numerical implementation

As mentioned earlier, the gel theory and its numerical implementation adopted in this study is mainly based on Hong *et al.* (2009) and Liu *et al.* (2011, 2013). A brief description is, however, included herein for completeness.

Consider a system which contains a network of polymers and a solvent, under mechanical loads and geometric constraints, and was held at a constant temperature. Define the reference state as the stress-free dry network, and let each small part of this network to be its corresponding coordinates X. Each part of the network would have a new coordinate $x_i(X)$ in deformed state. The deformation gradient of this network is defined as

$$F_{ik} = \frac{\partial x_i(X)}{\partial X_K} \tag{1}$$

As the deformation field $x_i(X)$ and distribution field $C(X)$ describe the state of the gel. For arbitrary variations of displacement field δx and concentration field δC, thermodynamics at equilibrium requires that

$$\int \delta W dV = \int B_i \delta x_i dV + \int T_i \delta x_i dA + \mu \int \delta C dV \tag{2}$$

W is the free-energy density of the gel that is a function of F, $C(X)$ is the nominal concentrations of the solvent molecules, $B_i(X)$ is the body force, $T_i(X)$ is the traction and μ is the chemical potential of the solvent molecules. Introduce a new free-energy function $\hat{W}$ expressed as

$$\hat{W} = W(F, C) - \mu C \tag{3}$$

Eq. (2) is simplified to a familiar form normally encountered in mechanics theory:

$$\int \delta \hat{W} dV = \int B_i \delta x_i dV + \int T_i \delta x_i dA \tag{4}$$

All molecules in a gel are assumed incompressible implying that the total volume of the gel is the sum of the volume of the dry system and the volume of the solvent and let ν be the volume of one solvent molecule.

$$1 + \upsilon C = detF \tag{5}$$

Following Flory and Rehner (1943), the free-energy function of the gel can be expressed as

$$\hat{W}(F, \mu) = \frac{1}{2} NkT(I - 3 - 2logJ) - \frac{kT}{\upsilon}\left[(J-1)log\frac{J}{J-1} + \frac{\chi}{J}\right] - \frac{\mu}{\upsilon}(J-1) \tag{6}$$

where N is the number of polymeric chains per reference volume, χ is a dimensionless measure of the enthalpy of mixing, $I=F_{ik}F_{ik}$ and $J=detF$. The condition of molecular incompressibility is imposed by substituting Eq. (5) into Eq. (6) to eliminate C. The chemical potential μ is normalized by kT and the nominal stress is normalized by kT/υ. A representative value of the volume per molecule is $\upsilon = 10^{-28} m^3$. At room temperature, $kT = 4 \times 10^{-21} J$ and $kT/\upsilon = 4 \times 10^7 Pa$. Two material parameters, $N\upsilon$ and χ, are introduced in the Flory-Rehner free-energy function. The value of $N\upsilon$ is in the range of $10^{-4} \sim 10^{-1}$ under small strain condition and the representative value of χ is $0 \sim 1.2$. Since χ is the dimensionless quantity that characterizing the interaction energy between polymers and solvent molecules, a lower value should be used if a large value of swelling ratio is desired.

When the network is dry, $\upsilon C=0$, the free-energy expressed in Eq. (6) is singular. A new reference state with $\upsilon C>0$ and state of free stress have to be adopted. The deformation gradient of the current state can be written as

$$F_{ik} = F'_{ij} F_{0ik} \tag{7}$$

F_{ik} and F'_{ij} are the deformation gradients of the current state with reference to the dry network and the current state related to the new reference state, F_{0jk} , respectively. Let $I' = F'_{ik}\ F'_{ik}$ and

Table 1 Mechanical properties of fruit and vegetable tissue

Living Tissues	Young's Modulus (MPa)
Lettuce	0.29 to 0.61
Potato	3.56 to 5.97
Fresh carrot (analytical)	2 to 33
Stoloniferous herbs (Trifolium repens/Potentilla reptans)	75 to 150
Flower stalk	106.1 to 384.5

J'=detF', the free-energy density and the nominal stress relative to the free-swelling state can be expressed as

$$\hat{W}'(F',\mu)=\frac{\lambda_0^{-3}}{2}NkT[\lambda_0^2 I'-3-2\log(\lambda_0^3 J')]-\frac{kT}{\upsilon}\left[(J'-\lambda_0^{-3})log\frac{J'}{\lambda_0^{-3}J'-1}+\frac{\chi}{\lambda_0^6 J'}\right]-\frac{\mu}{\upsilon}(J'-\lambda_0^{-3}) \tag{8}$$

This was implemented in the finite element program, ABAQUS, using a user-defined subroutine for a hyperelastic material with a temperature variable representing chemical potential (Hong *et al*. 2009). The properties of a gel material are described by the following three parameters: (i) $N\upsilon$ (the volume of polymeric chains), (ii) χ (the measure enthalpy mixing) and (iii) λ_0 (initial free-swelling stretch). Since $N\upsilon$ and χ are the parameters describing the properties of the polymers in gel, they are kept constant for the simulations of the same fruit. The initial stretch has to be larger than 1.0 to avoid singularity problem and preferably greater than 2.0 to ensure the desired relatively larger swelling ratio to mimic the growth of the fruits efficiently.

3. Growing patterns of fruits

A solids/shell system is established to mimic the pericarp/sarcocarp structure of each fruit. Various parts of a fruit are modeled using different types of materials as appropriate. Membrane core, if present in any fruit, is significantly stiffer than that of the sarcocarp and grows much less than both sarcocarp and pericarp. Elastic engineering materials of equivalent mechanical properties may be adopted to represent the stiff membrane while gel-based materials, with relatively equivalent mechanical properties to the natural plant materials to mimic the growth process of fruits, are employed to model the swelling of both sarcocarp and pericarp. Niklas (1989) reported that the value of Young's modulus of a plant tissue is affected by several factors including turgor pressure, geometry of its constituent cells and cell wall composition. He reported the values in the order of hundreds of MPa for Allium on sativum flower stalks with tissue density of about 0.15 g/cm^3. Georget *et al.* (2003) and Newman *et al.* (2005) reported the mechanical properties of several daily vegetables and fruits based on experiments. Hong *et al*. (2009) stated that the cross-linked polymers in the absence of solvent molecules have a shear modulus under the small-strain conditions as *NkT*, that is related to the value of Young's modulus *E*. Based on the above studies, the suggested values of Young's moduli of various living tissues are listed in Table 1. Unless stated otherwise in this study, the values of Young's modulus are listed in Table 2, and 0.33 is adopted for the Poisson's ratio of plant tissues. As different parts of fruits and vegetable grow at different paces (Dumais and Steele 2000), the phenomena can be simulated via varying the values of $N\upsilon$ and χ which inflects the swelling ratios of the gel materials (Liu *et al*. 2011, Wu *et al.*

Table 2 Analytical values of the Young's modulus adopted in this study

Tissues	Materials	Young's Modulus (MPa)
Mesophyll of leaves	Gel (*Nv*=0.005)	0.266
Sarcocarp of fruits	Gel (*Nv*=0.01)	0.532
Pericarp of fruits	Gel (*Nv*=0.1)	5.32
Membrane of fruits	Engineering	50
Vein of leaves	Engineering	300

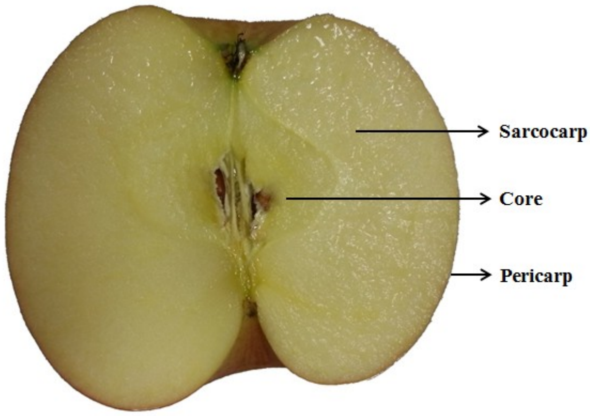

Fig. 1 Vertical cross-section of an apple

2013). In order to mimic the phenomena in a reasonable range, the values of χ of gel materials are set at 0.01 for mesophyll of leaves and sarcocarp of fruits and 0.1 for pericarp of fruits for gel materials in the simulations that follow.

The thickness of the pericarp and the ratio of major axis and minor axis of the models are prescribed proportionally, following the dimensions of a typical actual fruit. In the swelling implementation, the absolute values of chemical potential and those of other parameters are less crucial as the differential growth of each part has greater influence on the pattern formation of the fruits. Hence, in order to mimic the morphology of various fruits, the relative values of mechanical properties and chemical potential for core, sarcocarp and pericarp have to be judiciously selected.

3.1 Simulations of growth of apple

The first simulation involves the modeling of the growing of an apple which is a common solids/shell system fruit in nature. The vertical cross section of an actual apple as shown in Fig. 1 illustrates the three parts: core, sarcocarp and pericarp of an apple. Sketches of the details of finite element model of the above three parts are depicted in Fig. 2. For simplicity, the immature stage of apple is assumed to be spherical. The sarcocarp and pericarp of the apple grow significantly more and are relatively much softer than the core. Hence, it is reasonable to adopt gel material which is capable of large deformation for the sarcocarp and pericarp and engineering material which is relatively stiff to model the core. The top area of the core in the model is held stationary in three directions to mimic the presence of the stem there while the fruit deforms freely elsewhere.

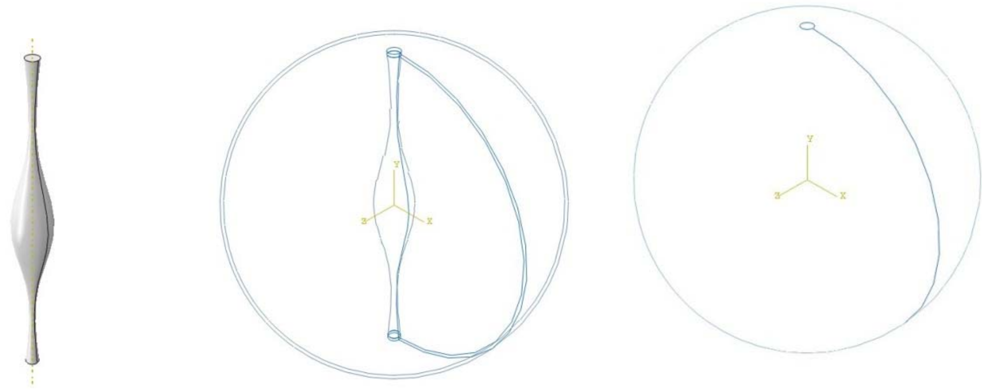

(a) (b) (c)

Fig. 2 Models for an apple, (a) core, (b) sarcocarp and (c) pericarp

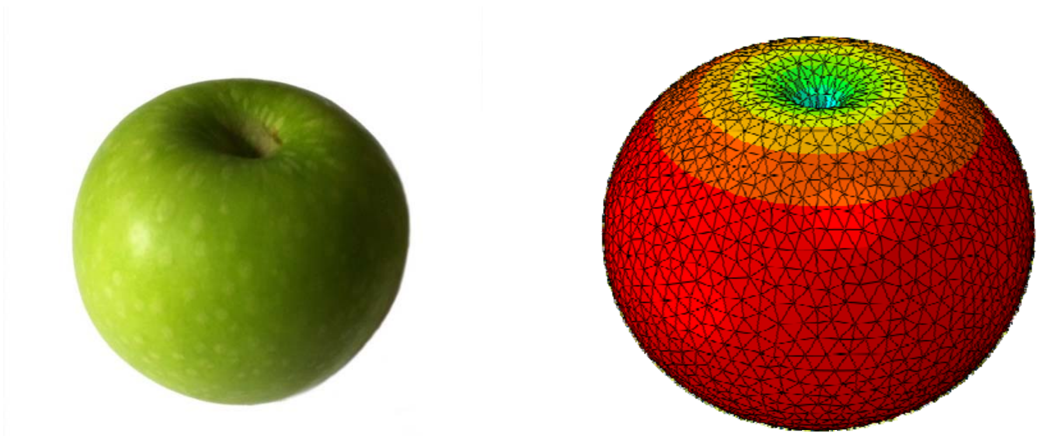

(a) (b)

Fig. 3 Comparison of (a) actual and (b) simulated configurations of apple at mature stage

Since engineering material properties are used for core, its deformation is normally negligible as compared to that of gel material. The growing process is simulated by varying the values of the gel chemical potential. The normalized values of the chemical potential in the sarcocarp vary from −0.0426 at the initial stage to 0 at the mature stage, whereas those of pericarp vary from the initial value of −0.00929 to 0 at the mature stage. The simulated apple will swell freely outwards, and eventually arrive at the configuration of the mature stage. Figs. 3 and 4 depict the comparison of actual and simulated configurations of an apple in the mature stage including those of vertical and horizontal cross sections. It is imperative to ensure the appropriate relative values of material properties with less concerns on actual values. Parameters affecting the growth geometry include (i) different core size and (ii) the values of $N\upsilon$ and χ of gel materials. Chemical potential values of gel materials and geometric constraints of membranes also play a significant role in the growth simulation of fruits.

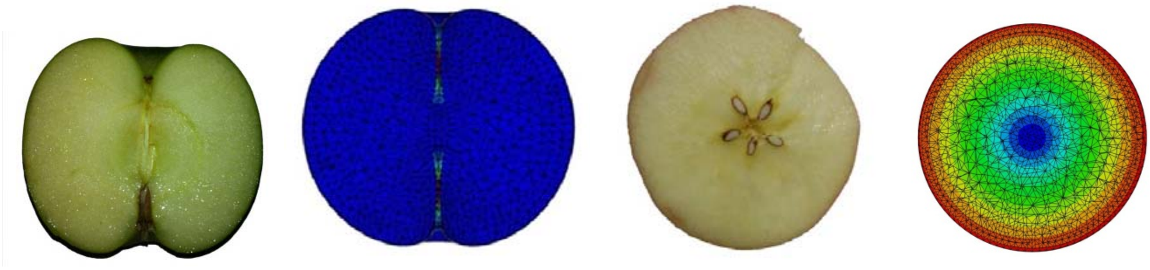

(a) (b) (c) (d)

Fig. 4 (a) Vertical and (c) horizontal cross-sectional configurations of actual apple as compared to those of (b) and (d) of simulated configurations at mature stage

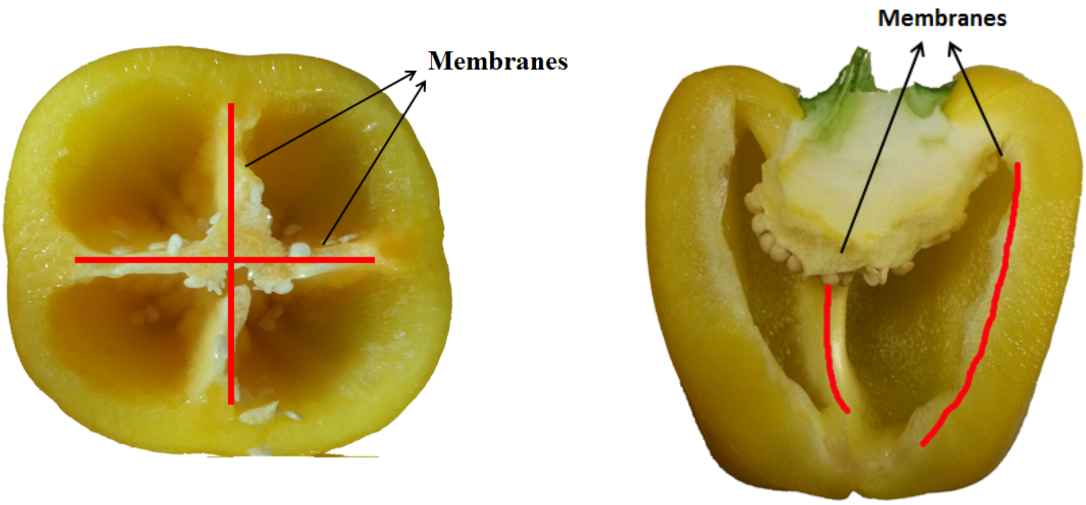

(a) (b)

Fig. 5 Locations of stiff membranes in capsicum, (a) horizontal and (b) vertical cross-sectional configurations

3.2 Simulations of growing patterns of capsicum

Capsicum is distinguished by its unique shape and internal structure. The core with seeds of the capsicum is rather spheroidal and located near the top connecting to the stem. There are four rather rigid membranes evenly distributed within the capsicum as shown in Fig. 5. Engineering material with the same properties mentioned earlier are used for both core and membranes as their stiffness are substantially higher than those of the sarcocarp and pericarp. The initial shape of the model is cylindrical trapezoid with the pin boundary conditions at the top to acknowledge the existence of the stem. The sarcocarp and pericarp are modeled as a thick shell structure using solid finite elements of gel material with the same properties adopted earlier for the simulation of apple, where the values of $N\upsilon$ are 0.01 and 0.1 respectively. The comparison between the actual capsicum and the simulated results are shown in Figs. 6-7.

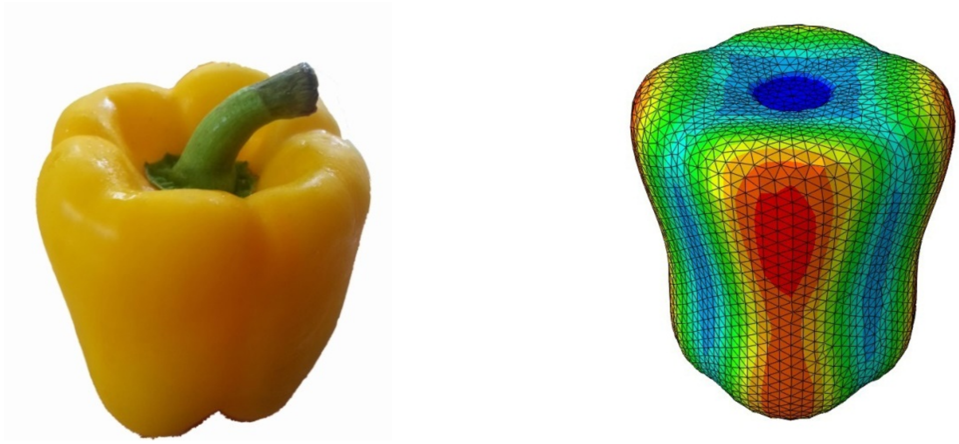

(a) (b)

Fig. 6 Comparison of (a) actual and (b) simulated configurations of capsicum at mature stage

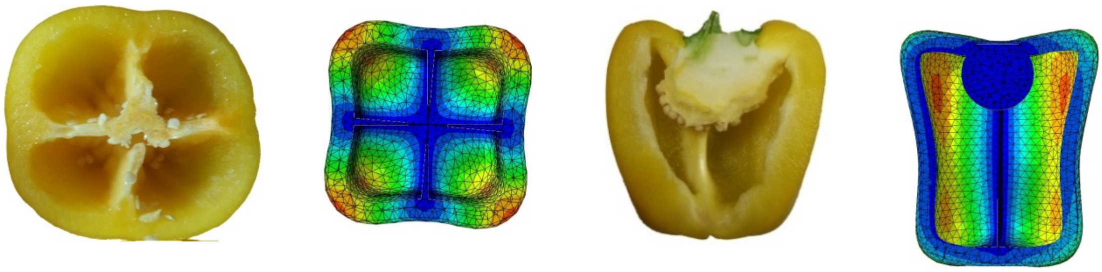

(a) (b) (c) (d)

Fig. 7 (a) Vertical and (c) horizontal cross-sectional configurations of actual capsicum as compared to those (b) and (d) of simulated configurations at mature stage

4. De-swelling of leaves

In order to mimic the drying process of leaves, the shapes at the mature stage of the leaves are used as the initial configurations. Leaves consist mainly of two parts: vein and mesophyll. As vein is much stiffer than mesophyll, only the latter is subjected to large deformation during the drying process. Engineering material properties are used for the vein whereas those of gel material are adopted for the mesophyll. In the implementation of de-swelling process, The initial chemical potential value assigned to the mesophyll is closer to zero than that of the final value to induce the shrinking of the gel materials to simulate the buckling deformation of the de-swelling leaves.

In order to investigate the drying process of leaves comprehensively, three starkly different types of leaves depicted in Fig. 8 are chosen for illustrated simulations. They are labeled from left to right as Leaf 1 (Ixora 'Super Pink'), Leaf 2 (Bauhinia Kockiana) and Leaf 3 (Epipremnum Aureum). The shapes of the leaves and their vein structures are modeled similar to those of the real leaves, as shown in Fig. 9. The simulated configurations are later compared with those of the same real leaves at their dried stage.

(a) (b) (c)

Fig. 8 Three different types of leaves used in the simulations, (a) Leaf 1 (Ixora 'Super Pink'), (b) Leaf 2 (Bauhinia Kockiana) and (c) Leaf 3 (Epipremnum Aureum)

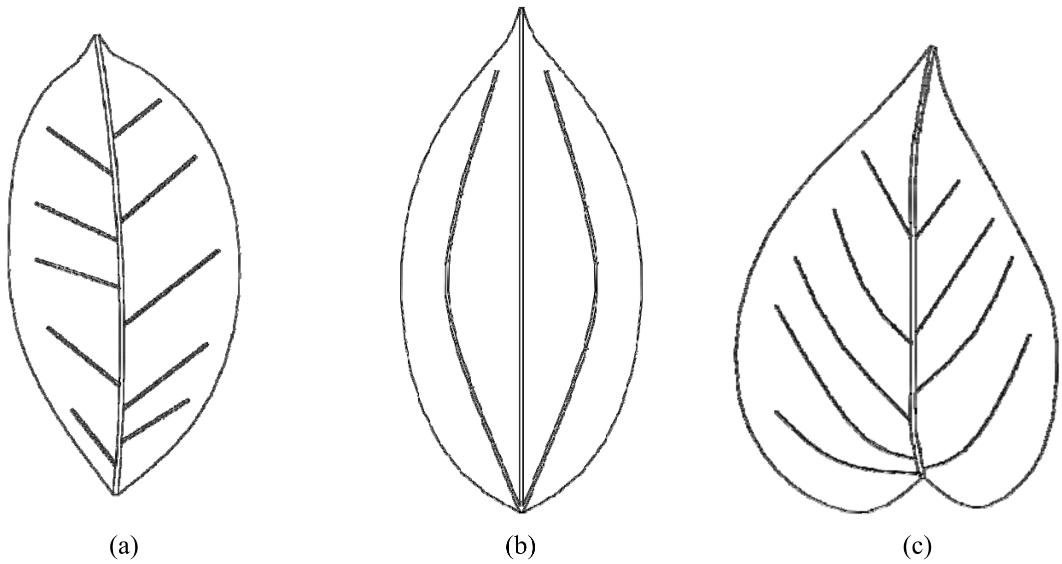

(a) (b) (c)

Fig. 9 Skeleton geometries of the three leaves in Fig. 9

Leaf 1 Ixora 'Super Pink'

The vein system of leaf 1 consists of a main vein in the middle with several sub-veins branched out representing a dicot leaf. The vein can be considered as the skeleton of the leaf and it is expected to have negligible shrinkage during its drying process. The engineering material properties are used for the vein system. Only the leaf base connecting to the stem is set to be fixed in three directions and hence the leaf is expected to experience a large bending deformation due to

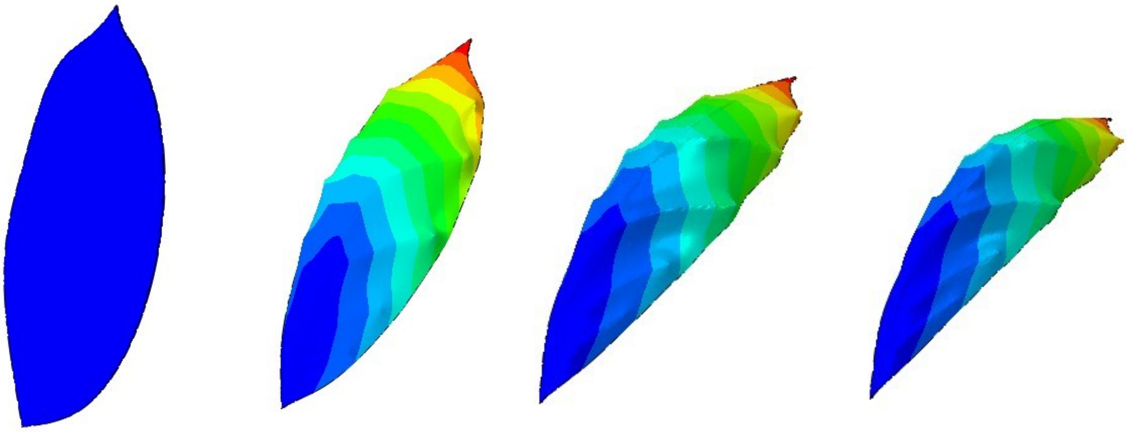

(a) (b) (c) (d)

Fig. 10 Simulated deformation patterns of leaf 1 during various stages of its drying process

(a) (b)

Fig. 11 Comparison of (a) actual and (b) simulated configurations of leaf 1 at dried stage

its fix-free boundary conditions. The initial value of the normalized chemical potential of the mesophyll is set at −0.000418 which is close to zero and is equivalent to that of the fresh leaf at the initial stage. The normalized chemical potential value reduces (alters to a larger negative value) during the de-swelling stages to the final value of −0.05237 to induce the shrinking of the gel materials to simulate the buckling deformation of the de-swelling leaf. During the simulation, the leaf model undergoes the de-swelling process until it is close to its dried state. Fig. 10 illustrates the simulated deformation patterns of leaf 1 during various stages of its drying process while the similarity of the actual and simulated leaf deformation patterns at its dried stage is depicted in Fig. 11.

Leaf 2 Bauhinia Kockiana

Different from leaf 1, in leaf 2 which is a monocot leaf, the vein system consists of three main longitudinal veins of similar sizes. Therefore, the properties of the three veins are set to be the same. They are relatively thinner than the one in leaf 1 and this has been reflected via adopting the smaller vein dimension of actual size in the simulated model. Similar to leaf 1, the drying process

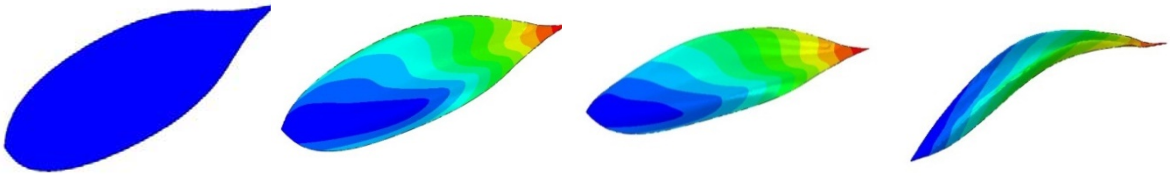

Fig. 12 Simulated deformation patterns of leaf 2 during various stages of its drying process

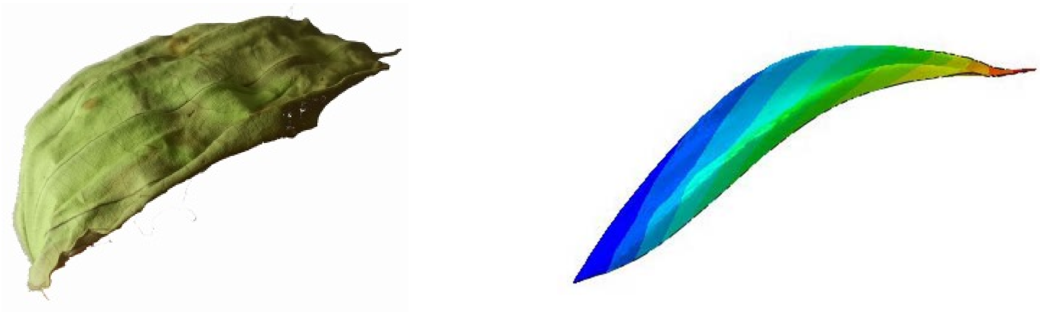

(a) (b)

Fig. 13 Comparison of (a) actual and (b) simulated configurations of leaf 2 at dried stage

is simulated by the de-swelling of the gel material in mesophyll. The initial value of the normalized chemical potential of the mesophyll is set at −0.0004188 for the fresh leaf at the initial stage. The value reduces during the de-swelling stages to the larger negative final value of −0.05237 inducing the shrinking of the gel materials. As the boundary conditions are the same as those for leaf 1, large displacement at the tip of the leaf is predicted while we expect less transverse deformation than that of leaf 1 due to the structural differences of their vein systems. Fig. 12 displays the simulated deformation patterns of leaf 2 at various stages of its drying process. We show the similarity of the actual and simulated leaf deformation patterns at its dried stage in Fig. 13.

Leaf 3 Epipremnum Aureum

The geometry and structure of leaf 3, which is a dicot leaf, as shown in Fig. 14, are markedly different from those of the previous two leaves. Though the vein system of leaf 3 seems to be similar to that of leaf 1, it is observed that the sub-veins of leaf 3 are substantially thinner than its main vein and those of the previous two leaves. In addition, the mesophyll of leaf 3 is relatively much stiffer than that of the previous two leaves, and hence the presence of the sub-veins of leaf 3 do not contribute significantly on the transverse stiffness of the leaf compared to the earlier two. In order to mimic such morphology, the reasonable vein sizes of main vein and sub-vein are adopted in order to match the actual dimensions. Similar to the simulations of the above 2 leaves, the drying process is simulated by the de-swelling of the gel material in mesophyll. The initial value of the normalized chemical potential of the mesophyll is set at −0.003219 and reduces (becomes larger negative) during the de-swelling stages to the final value of −0.042619 to induce the shrinking of the gel materials. The final transverse deformations at the edges are predicted to be large due to a substantial extension of mesophyll in the transverse direction and the presence of the

Fig. 14 Structure of Epipremnum Aureum for modelling

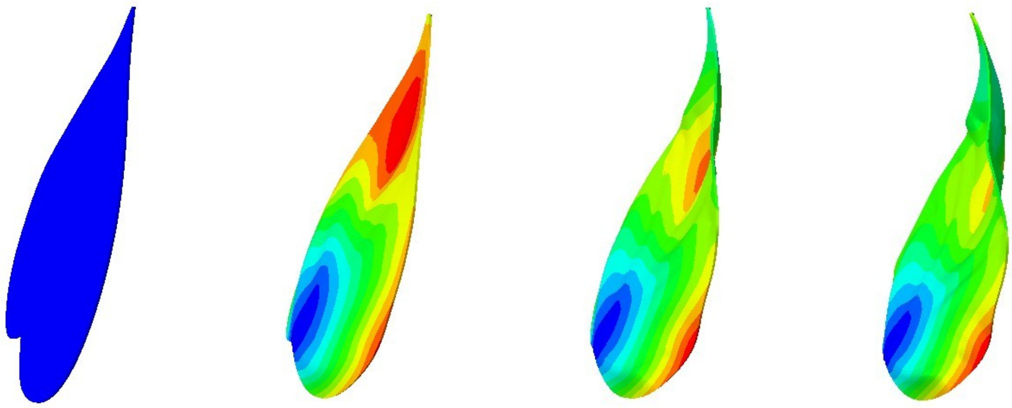

Fig. 15 Simulated deformation patterns of leaf 1 during various stages of its drying process

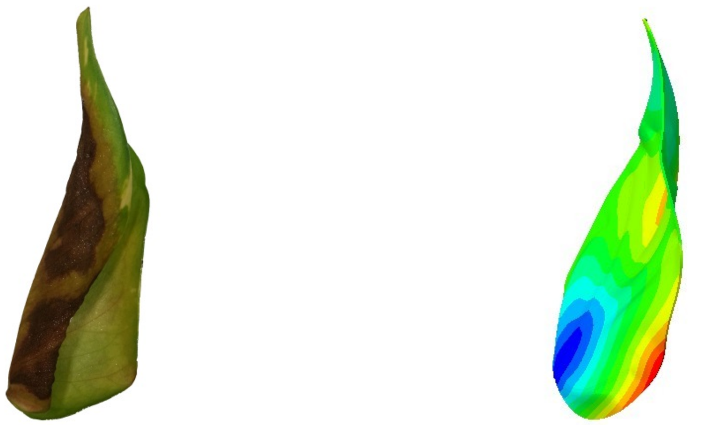

(a) (b)

Fig. 16 Comparison of (a) actual and (b) simulated configurations of leaf 3 at dried stage much less stiff sub-veins. Fig. 15 displays various simulated deformation patterns of leaf 3 during its drying process while the similarity of the actual and simulated dried leaf deformation patterns at the final stage is shown in Fig. 16.

From the pattern formations of the above three different kinds of leaves during their drying process, it can be concluded that the vein system plays a significant role in the leaf drying deformation patterns. During the drying process of the leaf, less displacements are expected at the tip or edges of the leaf with stiffer vein/s spanning in that direction while larger deformations are expected in less stiff direction and/or broader mesophyll extension.

5. Conclusions

In this article, we adopt the inhomogeneous field gel theory to mimic the formation patterns of the growing of natural fruits and drying of leaves via the swelling and de-swelling of gel materials. The study is focused mainly on numerical simulations of the systems with core/shell structures and thin membrane sheets. We adopt the swelling process of a gel material to simulate the growth of several types of common fruits with core/shell system, namely, apple and capsicum. For the drying process of leaves, three kinds of leaves with different vein structures and geometries are studied aiming for a more comprehensive investigation. The growing process of fruits and drying process of leaves are simulated using the inhomogeneous field theory of gel materials via ABAQUS finite element program. The study demonstrates that gel materials with proper material properties are suitable to represent the sarcocarp and pericarp in fruits and mesophyll in leaves for the simulation of the growth and drying processes of these natural produces with a view to explain their morphology.

Acknowledgements

Z.S. Liu is grateful for the support by National Natural Science Foundation of China under grant number 11242011 and number 11372236.

References

Censi, R., Di Martino, P., Vermonden, T. and Hennink, W.E. (2012), “Hydrogels for protein delivery in tissue engineering”, *J. Control. Rel.*, **161**(2), 680-692.

Chang, L.Y., Niu, Q.L., Miao, Y.B., He, S.P., Cui,C. and Huang, D.F. (2011), “Modeling study of fruit morphological formation in melon”, *Agricul. Sci. China*, **10**(5), 714-720.

Drury, J.L. and Mooney, D.J. (2003), “Hydrogels for tissue engineering: scaffold design variables and applications”, *Biomater.*, **24**(24), 4337-4351.

Dumais, J., and Steele, C.R. (2000), “New evidence for the role of mechanical forces in the shoot apical meristem”, *J. Plant Grow. Regul.*, **19**(1), 7-18.

Flory P.J. and Rehner J.J. (1943), “Statistical mechanics of cross-linked polymer networks II. swelling”, *J. Chem. Phys.*, **11**(11) 521-526.

Fujita, H. and Mochizuki, A. (2006), “The origin of the diversity of leaf venation pattern”, *Develop. Dyn.*, **235**(10), 2710-2721.

Georget, D.M.R., Smith, A.C. and Waldron, K.W. (2003), “Modelling of carrot tissue as a fluid-filled foam", *J. Mater. Sci.*, **38**, 1933-1938.

Givnish, T.J. (1987), "Comparative studies of leaf form: assessing the relative roles of selective pressures and phylogenetic constraints", *New Phytol*., **106**, 131-160.

Green, A.A., Kennaway, J.R., Hanna, A.I., Andrew Bangham, J. and Coen, E. (2010), "Genetic control of organ shape and tissue polarity", *PLoS Biology*, **8**(11), e1000537.

Hong, W., Liu, Z.S. and Suo, Z.G. (2009), "Inhomogeneous swelling of a gel in equilibrium with a solvent and mechanical load", *Int. J. Solid. Struct.*, **46**(17), 3282-3289.

Horkay, F. and McKenna, G. (2007), *Polymer Networks and Gels*, Physical Properties of Polymers Handbook, Springer, New York City, USA.

Kang, M.K. and Huang, R. (2010), "Swell-induced surface instability of confined hydrogel layers on substrates", *J. Mech. Phys. Solid.*, **58**, 1582-1598.

Kleverlaan, M., Van Noort, R.H. and Jones, I. (2005), "Deployment of swelling elastomer packers in shell E&P", *421-425, SPE/IADC Drilling, Conference*, Amsterdam, February.

Li, B., Cao, Y.P., Feng, X.Q. and Gao, H.J. (2012), "Mechanics of morphological instabilities and surface wrinkling in soft materials: a review", *Soft Matter*, **8**(21), 5728-5745.

Liu, Z.S., Hong, W., Suo, Z.G., Swaddiwudhipong, S. and Zhang, Y. (2010), "Modeling and simulation of buckling of polymeric membrane thin film gel", *Comput. Mater. Sci*., **49**(1 SUPPL), S60-S64.

Liu, Z.S. Swaddiwudhipong, S., Cui, F.F., Hong, W., Suo, Z.G. and Zhang, Y.W. (2011), "Analytical Solutions of Polymeric Gel Structures under Buckling and Wrinkle", *Int. J. Appl. Mech*., **3**(2) 235-257.

Liu, Z.S., Swaddiwudhipong, S. and Hong, W. (2013), "Pattern formation in plants via instability theory of hydrogels", *Soft Matter*, **9**(2), 577-587.

Newman, J.M., Hilton, H.W., Clifford, S.C. and Smith, A.C. (2005), "The mechanical properties of lettuce: A comparison of some agronomic and postharvest effects", *J. Mater. Sci*., **40**, 1101-1104

Niklas, K.J. (1989), "Mechanical behavior of plant tissues as inferred from the theory of pressurized cellular solids", *Am. J. Botany*, **76**(6), 929-937.

Wu, Z., Bouklas, N. and Huang, R. (2013), "Swell-induced surface instability of hydrogel layers with material properties varying in thickness direction", *Int. J. Solid. Struct*., **50**, 578-587.

Yin, J., Cao, Z., Li, C., Sheinman, I. and Chen, X. (2008), "Stress-driven buckling patterns in spheroidal core/shell structures", *Proc. Natl. Acad. Sci. USA*, **105**(49), 19132-19135.

Yin, J., Chen, X. and Sheinman, I. (2009), "Anisotropic buckling patterns in spheroidal film/substrate systems and their implications in some natural and biological systems", *J. Mech. Phys. Solid*., **57**(9), 1470-1484.